Diagnosis, Treatment Response, and Prognosis: The Role of ^{18}F-DOPA PET/CT in Children Affected by Neuroblastoma in Comparison with ^{123}I-mIBG Scan: The First Prospective Study

Arnoldo Piccardo[1], Giovanni Morana[2], Matteo Puntoni[3], Sara Campora[4], Stefania Sorrentino[5], Pietro Zucchetta[6], Martina Ugolini[7], Massimo Conte[5], Angelina Cistaro[1], Giulia Ferrarazzo[1], Marco Pescetto[8], Marco Lattuada[8], Gianluca Bottoni[1], Alberto Garaventa[5], Luca Giovanella*[9], and Egesta Lopci*[10]

[1]Department of Nuclear Medicine, Galliera Hospital, Genoa, Italy; [2]Neuroradiology Unit, IRCCS Istituto Giannina Gaslini, Genova, Italy; [3]Clinical Trial Research Unit, Galliera Hospital, Genoa, Italy; [4]Department of Oncology, Galliera Hospital, Genoa, Italy; [5]Unit of Pediatric Oncology, Istituto Giannina Gaslini, IRCCS, Genoa, Italy; [6]Department of Nuclear Medicine, University Hospital of Padova, Padova, Italy; [7]Medical Physics Department, Galliera Hospital, Genoa, Italy; [8]Anaesthesiology Department, Galliera Hospital, Genoa, Italy; [9]Clinic of Nuclear Medicine and Molecular Imaging, Imaging Institute of Southern Switzerland, Bellinzona and Lugano, Switzerland; and [10]Department of Nuclear Medicine, Humanitas Clinical and Research Hospital, IRCCS, Rozzano, Italy

Our purpose was to evaluate the diagnostic role of ^{18}F-3,4-dihydroxyphenylalanine (DOPA) PET/CT at the time of staging in children with neuroblastoma and to investigate its ability to assess treatment response. We also investigated the prognostic value of ^{18}F-DOPA PET/CT at the same time points. **Methods:** We enrolled children with neuroblastoma at onset. Before and after induction chemotherapy, all patients underwent ^{18}F-DOPA PET/CT and ^{123}I-metaiodobenzylguanidine (MIBG) scanning plus SPECT/CT. ^{18}F-DOPA PET/CT results were compared with those of ^{123}I-MIBG whole-body scanning (WBS). For each modality, patient-based analysis and lesion-based analysis were performed and sensitivity was calculated. We applied scoring systems to ^{123}I-MIBG scanning and ^{18}F-DOPA PET/CT (i.e.,^{123}I-MIBG WBS score and whole-body metabolic burden [WBMB], respectively) and evaluated the association between these parameters, the principal neuroblastoma risk factors, and outcome. **Results:** We enrolled 16 high-risk and 2 intermediate-risk neuroblastoma patients. On patient-based analysis, sensitivity in detecting primary tumors, soft-tissue metastases, and bone or bone-marrow metastases was 83%, 50%, and 92%, respectively, for ^{123}I-MIBG WBS versus 94%, 92%, and 100%, respectively, for ^{18}F-DOPA PET/CT. On lesion-based analysis, the sensitivity of ^{18}F-DOPA PET/CT in detecting soft-tissue and bone or bone-marrow metastases was 86% and 99%, respectively—significantly higher than that of ^{123}I-MIBG WBS, at 41% and 93%, respectively. After therapy, on patient-based analysis, the sensitivity in detecting primary tumors, soft-tissue metastases, and bone or bone-marrow metastases was 72%, 33%, and 38%, respectively, for ^{123}I-MIBG WBS versus 83%, 75% and 54%, respectively, for ^{18}F-DOPA PET/CT. On lesion-based analysis, the sensitivity of ^{18}F-DOPA PET/CT in detecting soft-tissue and bone or bone-marrow metastases was 77% and 86%, respectively—significantly higher than that of ^{123}I-MIBG WBS, at 28% and 69%, respectively. During follow-up, 8 cases of disease progression and 5 deaths occurred. On multivariate analysis, only posttherapeutic ^{18}F-DOPA WBMB (>7.5) was associated with progression-free survival. **Conclusion:** ^{18}F-DOPA PET/CT is more sensitive than ^{123}I-MIBG WBS in staging neuroblastoma patients and evaluating disease persistence after chemotherapy. In a time-to-event analysis, posttherapeutic ^{18}F-DOPA WBMB remained the only risk factor associated with disease progression.

Key Words: PET/CT; DOPA; neuroblastoma; chemotherapy; prognosis

J Nucl Med 2020; 61:367–374
DOI: 10.2967/jnumed.119.232553

High-risk neuroblastoma, commonly defined by metastatic disease in patients older than 12–18 mo (*1,2*), by protooncogene MYCN amplification in patients at any age, and by unfavorable histopathologic features (*3,4*), displays long-term survival rates of approximately 40% (*5–7*). Internationally agreed-upon treatment options for high-risk neuroblastoma (NB-AR-01 protocol) include multiagent induction chemotherapy, surgery, high-dose chemotherapy followed by autologous stem cell transplantation, external-beam radiotherapy, radionuclide therapy, differentiation therapies, and immunotherapy (*8*). A complete response to induction chemotherapy, as evaluated by various diagnostic procedures (e.g., imaging or bone-marrow biopsy), is one of the main early prognostic factors in high-risk neuroblastoma.

^{123}I-metaiodobenzylguanidine (MIBG) scintigraphy has long been recognized as the main imaging procedure for staging of neuroblastoma. More recently, the International Society of Paediatric Oncology European Neuroblastoma (SIOPEN) identified the SIOPEN semiquantitative ^{123}I-MIBG skeletal scoring system (SIOPEN Method 3) as an excellent inter- and intraobserver method that can estimate the extension of bone or bone-marrow metastases in a reproducible way, thereby providing a reliable prognostic indicator in neuroblastoma (*9*). In addition, SIOPEN Method 3 was validated as a prognostic response predictor in 2 independent trial populations (*8*). More specifically, a postinduction skeletal score greater than 3 identifies patients with a very poor prognosis who require different treatment strategies (*9*). On the other hand,

Received Jun. 18, 2019; revision accepted Aug. 12, 2019.
For correspondence or reprints contact: Arnoldo Piccardo, Department of Nuclear Medicine, E.O. Ospedali Galliera, Mura delle Cappuccine 14, 16128 Genoa, Italy.
E-mail: arnoldo.piccardo@galliera.it
*Contributed equally to this work.
Published online Sep. 20, 2019.

^{123}I-MIBG scintigraphy is cumbersome (*10*), requiring proper patient preparation and correct recognition of the distribution pattern, and is frequently limited by the difficult anatomy in children and low-quality images (*11*). Various PET tracers have been tested as effective substitutes for ^{123}I-MIBG in assessing neuroblastoma (*12*), and ^{18}F-3,4-dihydroxyphenylalanine (DOPA) (*13*), radiolabeled somatostatin analogs (*14,15*), and ^{124}I-MIBG have proved the most promising (*16*). ^{18}F-DOPA PET/CT has already proved to be more sensitive than ^{123}I-MIBG scanning in patients with neuroblastoma relapse (*17*). Specifically, ^{18}F-DOPA PET/CT has been demonstrated to be a reliable diagnostic procedure in detecting small soft-tissue and bone or bone-marrow metastases that are not accurately detected by ^{123}I-MIBG scintigraphy (*17,18*). In addition, this imaging procedure has shown better diagnostic results than conventional procedures (i.e., CT and MRI), disclosing more neuroblastoma localizations in bone marrow and lymph nodes and more soft-tissue recurrences (*19*). Direct comparison with ^{18}F-FDG PET/CT has also shown that ^{18}F-DOPA PET/CT is the most sensitive and accurate method of identifying neuroblastoma localizations, whether metastases or primary tumors (*20*). Moreover, its prognostic role at the time of recurrence has already been validated by means of an adequate whole-body scoring system, defined as whole-body metabolic burden (WBMB), which is able to evaluate disease extension (*18*). In this context, the possibility of disease progression and death has been seen to increase in proportion to the WBMB value (with a cutoff value of $>$7.5) (*18*). However, ^{18}F-DOPA PET/CT has never been tested as a pivotal diagnostic tool for staging of patients affected by neuroblastoma and evaluation of treatment response to induction chemotherapy. Indeed, this diagnostic PET-based approach could help in stratifying patients after induction chemotherapy and identify subjects at different risks of disease persistence or recurrence. The proven ability of ^{18}F-DOPA PET/CT to detect small metastases could be even more important when evaluating disease persistence.

The primary aim of this study was to evaluate the diagnostic role of ^{18}F-DOPA PET/CT at the time of first diagnosis in children with neuroblastoma. We also investigated the ability of this procedure to assess response to chemotherapy. Lastly, we evaluated the prognostic role of ^{18}F-DOPA PET/CT in high-risk neuroblastoma patients on diagnosis and after induction chemotherapy by testing the relationship between WBMB, progression-free survival (PFS), and overall survival (OS).

MATERIALS AND METHODS

The local ethics committee and the Agenzia Italiana del Farmaco, a public agency of the Italian Ministry of Health, approved the study. Written informed consent was obtained from all subjects. The trial was registered in the European Clinical Trial Database (EudraCT number 2012-005398-30).

Patient Population

From December 2013 to January 2017, we prospectively enrolled neuroblastoma patients who were candidates for SIOPEN therapeutic protocols and referred for imaging procedures to the Nuclear Medicine Department of Galliera Hospital. Before and within 7 d after chemotherapy, all patients underwent both ^{18}F-DOPA PET/CT and ^{123}I-MIBG whole-body scanning (WBS) with additional SPECT. The imaging procedures were performed within 10 d of each other (range, 1–10 d; mean, 4.1 d; SD, ±3.3 d).

The inclusion criteria were histologically proven neuroblastoma at the time of first diagnosis (age $>$ 12 mo and $<$ 18 y), no previous chemotherapy, and written informed consent. The exclusion criteria were comorbidity due to other neoplasms, known hypersensitivity to the active ingredient or excipients contained in the radiopharmaceuticals, and any other medical condition contraindicating the study in the investigator's judgment.

Imaging Modalities

^{123}I-MIBG scintigraphy and ^{18}F-DOPA PET/CT were performed on fasting patients within 10 d of each other; no treatment was administered between the 2 scans. Images were acquired according to standard procedures (*10*).

Whole-body ^{18}F-DOPA PET/CT was performed 60 min after tracer injection according to our previous experience (*10,17–19*). The activity administered was calculated according to the patient's body weight (4 MBq/kg), with a minimum activity of 80 MBq (range, 80–185 MBq; mean, 110 MBq; SD, ±35 MBq).

^{123}I-MIBG scans were acquired 24 h after injection of the tracer by means of a dual-head γ-camera (Millennium; GE Healthcare). The activity administered was calculated according to the patient's body weight, with a minimum activity of 80 MBq, as suggested by Lassmann et al. (range, 80–185 MBq; mean, 110 MBq; SD, ±35 MBq) (*21*). Spot views of the various body segments were acquired. Each spot view was acquired for a maximum of 10 min (~500 kilocounts; 100 kilocounts for spot views of the lower limbs). Thoracoabdominal SPECT was performed on all patients at intervals of 24 h, as suggested by Matthay et al. (*22*) and Olivier et al. (*23*). Fused SPECT/CT images were analyzed on a dedicated workstation (Xeleris; GE Healthcare) that allowed coregistration of ^{123}I-MIBG and CT images previously acquired during the PET/CT examination.

Image Interpretation

Two expert nuclear medicine physicians interpreted separately ^{18}F-DOPA PET/CT and ^{123}I-MIBG SPECT/CT. They were aware of the patient's clinical history and anatomical imaging modalities (i.e., MRI/CT) but blinded to any ^{18}F-DOPA PET/CT or ^{123}I-MIBG SPECT/CT results, respectively. Finally, a consensus review of discordant findings was done.

On ^{18}F-DOPA PET/CT or ^{123}I-MIBG SPECT/CT, any focal, nonphysiologic uptake higher than that of the surrounding background was considered pathologic (*17,18*). The 2 readers analyzed the whole-body images by focusing on primary tumors (abdominal or thoracic), lymph nodes, lungs, liver, bone, and brain. Both studies were interpreted on a patient-by-patient basis (patient-based analysis) and a lesion-by-lesion basis (lesion-based analysis) before and after chemotherapy. In patient-based analysis, the detection rate (DR) was defined as the ability to detect at least 1 pathologic finding in each subject. In lesion-based analysis, the DR was defined as the ability to detect suspected lesions in relation to the total number of lesions detected by both tracers and by anatomic imaging modalities.

Scoring Systems

The effectiveness of ^{123}I-MIBG and ^{18}F-DOPA PET/CT in detecting neuroblastoma was assessed by reviewing the uptake patterns for each radiopharmaceutical in the following locations: primary tumor, local and regional soft-tissue metastases, and bone and bone-marrow metastases. SIOPEN Method 3 was applied to the ^{123}I-MIBG scans to evaluate disease extent in the bone and bone marrow (*8*). To semiquantify soft-tissue neuroblastoma localizations, the modified Curie scoring system was applied, based on the methodology of Matthay et al. (soft-tissue^{123}I-MIBG score) (*18,24*).

Another scoring system, the WBMB, was applied to ^{18}F-DOPA PET/CT images to evaluate the extent of bone or bone-marrow involvement and that of primary tumor and of soft-tissue metastases (*18*). Specifically, for ^{18}F-DOPA PET/CT, SIOPEN Method 3 was applied to evaluate the extent of bone and bone-marrow disease. To

better characterize the intrinsic metabolic burden of each bone segment, we multiplied the SUV_{mean} by the score of each bone segment. The whole-body bone metabolic burden was calculated as the sum of the bone-segment metabolic burden of each bone segment in the PET image. To determine the extent and load of soft-tissue recurrence or metastases, a whole-body soft-tissue metabolic burden was applied per patient (*18,25*). For each tumor lesion, the soft-tissue metabolic burden was calculated as SUV_{mean} multiplied by tumor volume. Tumor volume was obtained from the CT images of the PET/CT acquisitions (*26*). The whole-body soft-tissue metabolic burden was calculated as the sum of the metabolic burden of each tumor lesion in the PET image. Finally, the overall WBMB was calculated as the sum of whole-body bone metabolic burden plus whole-body soft-tissue metabolic burden.

Risk Stratification

Each patient was risk-stratified according to age at the time of diagnosis (≤18 mo or >18 mo), histopathologic results, stage (3 or 4), MYCN amplification, lactate dehydrogenase level, homovanillic and vanilmandelic acid levels, ^{123}I-MIBG score before and after induction chemotherapy, and WBMB before and after induction chemotherapy.

At final follow-up, patients were deemed to be disease-free if they had less than 10 mm of residual soft tissue at the primary site and in nonprimary lesions and complete resolution of ^{123}I-MIBG uptake (*27*).

Patients were considered to have disease persistence or partial response if there was a decrease by more than 30% at the primary and nonprimary sites and if ^{123}I-MIBG uptake at the primary site was stable, improved, or resolved and there was more than a 50% reduction in ^{123}I-MIBG absolute bone score (*27*).

Disease was considered to have progressed if there was a 20% increase in longest lesion diameter or any new soft-tissue or bone lesions detected by CT/MRI that were also ^{123}I-MIBG–avid or were biopsied and confirmed to be neuroblastoma (*27*).

Standard of Reference

Although only DRs were calculated for each diagnostic modality, we applied a standard of reference, which was able to provide some confirmation of the site of disease. The standard of reference for the primary tumor was based on histopathology results (available for all patients). The standard of reference for soft-tissue metastases was based on histopathology results or on diagnostic contrast-enhanced CT or MRI findings (available for all patients). The gold standards for bone and bone-marrow metastases were bone-marrow biopsy (available for all patients), CT, or MRI (available for all patients). A median clinical and imaging follow-up of 29.3 mo (range, 19–53 mo) was available for each patient.

Clinical decisions after induction chemotherapy were based on the results of ^{123}I-MIBG WBS and conventional radiologic imaging (i.e., CT and MRI), not the results of ^{18}F-DOPA PET/CT.

Statistical Analysis

Descriptive statistics included mean, SD, and range for data involving continuous factors and scores; in the case of categoric factors, we used absolute and relative frequencies, along with percentage. The Spearman rank correlation coefficient was adopted to test the correlation between ^{123}I-MIBG SPECT/CT and ^{18}F-DOPA PET/CT scores. For diagnostic analyses, DRs, defined as the percentage of positive subjects (in patient-based analysis) or lesions (in lesion-based analysis), were calculated for each diagnostic modality at each site of disease. We adopted the exact McNemar test to compare DRs between diagnostic modalities. For prognostic analyses, we used Kaplan–Meier estimates of the cumulative probability of PFS and OS, defined as the interval between initial diagnosis and the onset of disease persistence/progression or death, and we tested the difference between time-to-event curves by means of the log-rank test. Cox proportional-hazards modeling was used to estimate the risk of disease persistence/progression and death from any cause, adjusting for age and other factors that proved to be associated with PFS and OS on univariate analyses. Since ^{123}I-MIBG SPECT/CT and ^{18}F-DOPA PET/CT scores were highly correlated, we used different models for each score to avoid collinearity and to test their independent association with PFS and OS. All analyses were conducted using Stata software (version 14.2; StataCorp.). Two-tailed probabilities are reported, and a P value of 0.05 was used to define nominal statistical significance.

RESULTS

We enrolled 16 high-risk and 2 intermediate-risk patients; their main characteristics are summarized in Table 1. For clinical reasons, the 2 intermediate-risk patients and 1 of the high-risk patients underwent not NB-AR-01 but different therapeutic protocols with different schemes of induction therapy; they were therefore included only in the diagnostic analysis and were excluded from the prognostic analysis (Table 1).

At the time of first staging, ^{123}I-MIBG SPECT/CT proved positive in 17 of 18 patients, whereas ^{18}F-DOPA PET/CT was positive in all 18 patients. On patient-based analysis, the DR in detecting primary tumors, soft-tissue metastases, and bone or bone-marrow metastases was 83%, 50%, and 92%, respectively, for ^{123}I-MIBG SPECT/CT versus 94%, 92%, and 100%, respectively, for ^{18}F-DOPA PET/CT (Fig. 1; Table 2). On lesion-based analysis, the DR of ^{18}F-DOPA PET/CT in detecting soft-tissue and bone or bone-marrow metastases was 86% and 99%, respectively—significantly higher ($P < 0.001$) than that of ^{123}I-MIBG SPECT/CT, at 41% and 93%, respectively (Fig. 2; Table 3).

After induction chemotherapy, ^{123}I-MIBG SPECT/CT proved positive in 14 of 18 neuroblastoma patients, whereas ^{18}F-DOPA PET/CT was still positive in 17 patients. However, when the analysis did not consider primary tumors but only metastatic sites of disease, ^{123}I-MIBG SPECT/CT proved positive in only 8 patients; by contrast, ^{18}F-DOPA PET/CT was still positive in 15.

On patient-based analysis, the DR in detecting primary tumors, soft-tissue metastases, and bone or bone-marrow metastases was 72%, 33%, and 38%, respectively, for ^{123}I-MIBG SPECT/CT versus 83%, 75%, and 54%, respectively, for ^{18}F-DOPA PET/CT (Table 2). On lesion-based analysis, the DR of ^{18}F-DOPA PET/CT in detecting soft-tissue and bone or bone-marrow metastases was 77% and 86%, respectively—significantly higher than that of ^{123}I-MIBG SPECT/CT, at 28% and 69%, respectively ($P < 0.001$ and $P = 0.001$, respectively) (Table 3; Fig. 3).

Over a median follow-up of 29.3 mo (interquartile range, 19.0–53.1 mo), among the 15 patients considered in the prognostic analysis, 8 cases of disease progression and 5 deaths occurred. Kaplan–Meier PFS curves showed that only initial stage (stage 3 vs. 4) and the ^{18}F-DOPA WBMB measured after induction chemotherapy (WBMB > 7.5; Fig. 4) were associated with prognosis. However, an important trend toward significance was also observed between outcome and pretherapy ^{123}I-MIBG WBS (≥46), pretherapy ^{18}F-DOPA WBMB (≥45; Fig. 4), and homovanillic acid levels (≥32 μmol/mmol creatinine) measured before therapy. Finally, risk estimates (unadjusted and adjusted) for disease progression were also calculated from the Cox model. After adjustment for all risk factors showing at least a trend toward significance at the univariate level, ^{18}F-DOPA WBMB evaluated after induction chemotherapy was the only factor independently

TABLE 1
Main Clinical, Histopathologic, and Biochemical Features of Patients (n = 18)

Feature	Data
Age (mo)	34 ± 19 (12–72)
Sex, male	12 (67)
Histopathology	
Undifferentiated	6 (33)
Poorly differentiated	9 (50)
Unknown	3 (17)
Stage	
3	4 (22)
4	14 (78)
Treatment	
NB AR 01	15 (83)
LINES/personalized	2/1 (17)
MYC amplification	10 (56)
Lactate dehydrogenase (UI/L), median (IQR)	median, 2,890 (IQR, 1,506–5,275)
Homovanillic acid levels (μmol/mmol creatinine), median (IQR)	median, 66.7 (IQR, 32.0–76.6)
Vanilmandelic acid levels (μmol/mmol creatinine), median (IQR)	median 26.1 (IQR, 5.3–123.9)
^{18}F-DOPA WBMB score	
Before induction chemotherapy	191.9 ± 349.1 (0–1,120)
After induction chemotherapy	18.2 ± 43.1 (0–169)
^{123}I-MIBG WBS score	
Before induction chemotherapy	24.7 ± 20.9 (0–58)
After induction chemotherapy	3.6 ± 9.9 (0–42)

Continuous data are mean ± SD followed by range in parentheses; count data are number followed by percentage in parentheses (unless otherwise noted).
LINES = Low and Intermediate Risk Neuroblastoma European Study; IQR = interquartile range.

and directly associated with PFS. More specifically, patients with a ^{18}F-DOPA WBMB score higher than 7.5 displayed a significantly higher risk of disease progression than those with a score of 7.5 of less (hazard ratio, 10.7; 95% confidence interval, 1.09–104.8; P = 0.041). No significant association was found between the risk factors considered and OS.

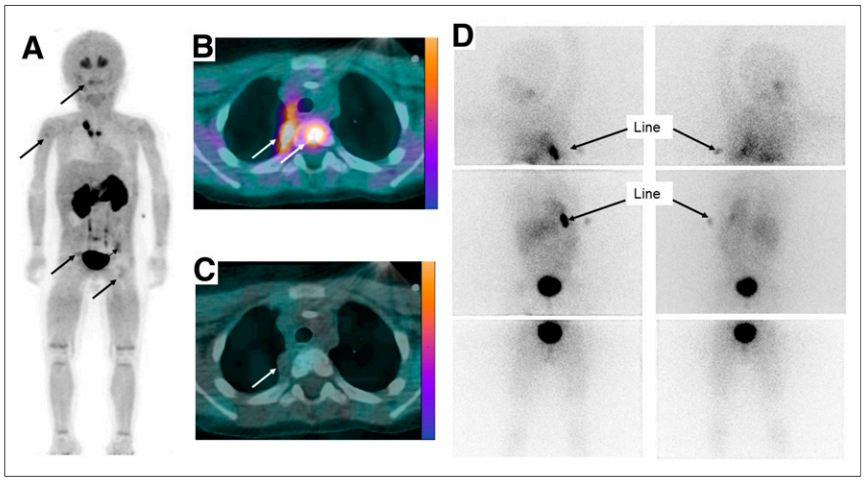

FIGURE 1. A 3-y-old child with stage 4 neuroblastoma (MYCN-amplified) of thoracic primary. (A and B) ^{18}F-DOPA PET/CT (maximum-intensity projection [A] and axial image [B]) showed intense uptake in primary tumor and identified some bone and bone-marrow metastases (arrows). (C and D) ^{123}I-MIBG WBS with additional SPECT/CT (axial image [C] and anterior and posterior views [D]) did not identify any site of pathologic uptake.

Of the 9 patients with completely negative findings on ^{123}I-MIBG WBS and persistently positive ^{18}F-DOPA WBMB after induction chemotherapy, 3 showed persistence or progression of disease at the end of treatment. However, the 6 patients who did not develop disease progression had an ^{18}F-DOPA WBMB value no higher than 1. All 5 patients with a WBMB higher than 7.5 after induction chemotherapy developed persistence or progression of disease, whereas only 2 of the 10 patients with a WBMB lower than 7.5 developed persistence or progression of disease (Supplemental Fig. 1; supplemental materials are available at http://jnm.snmjournals.org). By contrast, although a ^{123}I-MIBG WBS score higher than 3 identified 3 patients who showed disease persistence or progression, 4 (33%) of the 12 patients with a ^{123}I-MIBG WBS score of 3 or less developed disease persistence or progression (Fig. 5). Thus,

TABLE 2
DRs for Patient-Based Analysis

Timing	^{123}I-MIBG SPECT/CT	^{18}F-DOPA PET/CT	*P**
Before induction chemotherapy			
Primary tumors	15 (83%)	17 (94%)	0.5
Soft-tissue metastases	6 (50%)	11 (92%)	0.06
Bone or bone-marrow metastases	12 (92%)	13 (100%)	1.0
After induction chemotherapy			
Primary tumor	13 (72%)	15 (83%)	0.6
Soft-tissue metastases	4 (33%)	9 (75%)	0.06
Bone or bone-marrow metastases	5 (38%)	7 (54%)	1.0

*Exact McNemar significance probability.

DRs (%) were calculated for each single diagnostic modality at each site of disease. Denominator for DRs on primary tumors is total number of patients (n = 18), considering that all are subjects with established cancer. For evaluations on soft-tissue and bone or bone-marrow lesions, denominator is maximum number of patients found to be positive by 2 diagnostic modalities (n = 12 for soft tissue; n = 13 for bone or bone-marrow lesions).

^{123}I-MIBG WBS and ^{18}F-DOPA WBMB scores were positively correlated only before induction chemotherapy (before: Spearman $\rho = 0.61$, $P = 0.007$; after: $\rho = 0.38$, $P = 0.11$). Specifically, ^{18}F-DOPA WBMB showed greater dispersion than ^{123}I-MIBG WBS, displaying an interquartile range of 20–128 before chemotherapy and 1–9 after chemotherapy, versus respective ranges of 2–42 and 0–2 for ^{123}I-MIBG (Supplemental Fig. 2).

DISCUSSION

First, we found that ^{18}F-DOPA PET/CT was more sensitive than ^{123}I-MIBG scanning in detecting neuroblastoma localizations in a well-selected population of neuroblastoma children analyzed at the time of first diagnosis, as proved by comparing PET/CT and ^{123}I-MIBG SPECT/CT images of all patients. This finding is of particular interest, as in the 2 previous studies comparing ^{18}F-DOPA and ^{123}I-MIBG (*17,20*), SPECT/CT images were unavailable. In our study, ^{18}F-DOPA PET/CT was even more sensitive in detecting soft-tissue metastases and small bone or bone-marrow localizations.

Second, we found that ^{18}F-DOPA PET/CT was a reliable diagnostic tool for evaluating treatment response after induction chemotherapy and provided important information on disease persistence. Specifically, ^{18}F-DOPA PET/CT proved to be more sensitive than ^{123}I-MIBG SPECT/CT in disclosing small and faint persistent bone and bone-marrow foci of pathologic uptake after chemotherapy. However, it would have been difficult to ascertain the real clinical impact of this finding if we had not tested the prognostic role of ^{18}F-DOPA PET/CT. In other words, the real issue is whether the higher number of lesions disclosed by ^{18}F-DOPA PET/CT after induction chemotherapy was associated with a higher probability of disease persistence or progression at the end of follow-up or whether the higher number of lesions was a simple and futile expression of diagnostic sensitivity. Accordingly, we evaluated the prognostic value of ^{18}F-DOPA PET/CT both at the time of disease onset and after induction chemotherapy. To better understand each patient's risk, we semiquantified the disease burden by using the previously validated ^{18}F-DOPA WBMB (*18*) and compared this with the ^{123}I-MIBG WBS and the other recognized prognostic factors. Both scores measure the burden of the disease, excluding the primary tumor. So far, no reliable and validated methods have been used to quantify the extension and activity of the primary tumor on ^{123}I-MIBG SPECT/CT (*8,10*) and ^{18}F-DOPA PET/CT images. In this regard, we found that, at the univariate level, only disease stage on initial diagnosis (stage 3 vs. stage 4) and WBMB measured after induction chemotherapy (WBMB > 7.5) were associated with prognosis. Notably, neither MYCN amplification nor a ^{123}I-MIBG score higher than 3 after chemotherapy was significantly associated with PFS. By contrast, a marked disease burden documented at the time of first diagnosis by means of ^{123}I-MIBG scanning (^{123}I-MIBG WBS > 46) and ^{18}F-DOPA PET/CT (WBMB ≥ 45) showed an important trend toward significance ($P = 0.06$ and $P = 0.08$, respectively). This finding seems to be in line with what was reported in a recent paper by Lewington et al. (*9*), who showed that patients with a SIOPEN score higher than 48 at the time of first diagnosis had a significantly lower response rate to induction chemotherapy than patients with a SIOPEN score of 48 or less.

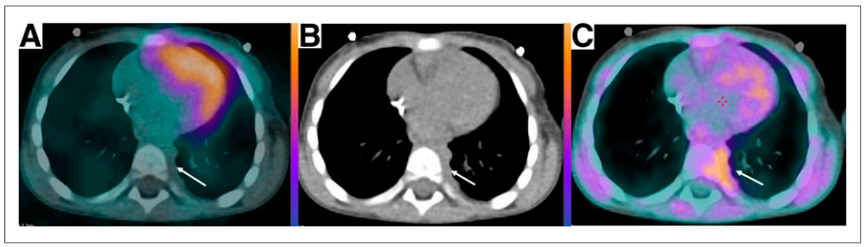

FIGURE 2. A 3-y-old child with stage III neuroblastoma (MYCN-amplified) of abdominal primary. On axial images, suggestive left paravertebral nodules detected on contrast-enhanced CT were negative on ^{123}I-MIBG SPECT/CT (A and B) but positive on ^{18}F-DOPA PET/CT (B and C).

However, the Cox models showed that only an ^{18}F-DOPA PET/CT WBMB score

TABLE 3
DRs for Lesion-Based Analysis

Timing	^{123}I-MIBG SPECT/CT	^{18}F-DOPA PET/CT	*P**
Before induction chemotherapy			
Soft-tissue metastases	20 (41%)	42 (86%)	<0.001
Bone or bone-marrow metastases	494 (93%)	522 (99%)	<0.001
After induction chemotherapy			
Soft-tissue metastases	11 (28%)	30 (77%)	<0.001
Bone or bone-marrow metastases	54 (69%)	67 (86%)	0.001

*Exact McNemar significance probability.

DRs (%) were calculated for each single diagnostic modality at each site of disease. Denominator for DRs is maximum number of lesions found to be positive by 2 diagnostic modalities: $n = 49$ and $n = 39$ before and after induction chemotherapy, respectively, for soft tissue; $n = 529$ and $n = 78$ before and after induction chemotherapy, respectively, for bone or bone-marrow lesions.

higher than 7.5 measured after induction chemotherapy was associated with PFS. This cutoff had already been validated by our previous study (*18*), in which patients with a WBMB score higher than 7.5 at the time of neuroblastoma relapse had a higher probability of disease progression and death. In the present study, we found that, of the 9 patients with negative ^{123}I-MIBG WBS results and persistent positive ^{18}F-DOPA WBMB results after induction chemotherapy, 3 had disease persistence or progression at the end of follow-up. All 3 of these patients showed at least 4 persistent disease localizations on ^{18}F-DOPA PET/CT, and in 2 patients the disease burden measured by means of WBMB was scored at higher than 7.5.

In addition, all 5 patients with ^{18}F-DOPA WBMB scores higher than 7.5 after induction therapy showed disease persistence or progression regardless of their ^{123}I-MIBG WBS score. From this point of view, ^{18}F-DOPA WBMB was the most accurate parameter in stratifying the risk of high-risk neuroblastoma patients after induction chemotherapy. We could speculate that a greater use of sensitive PET tracers, such as ^{18}F-DOPA, could identify patients at very high risk for whom a more intense therapeutic regimen is warranted.

This study has some limitations: its low statistical power (low number of patients and events) and the fact that the effects of different therapies performed after induction therapy were not considered

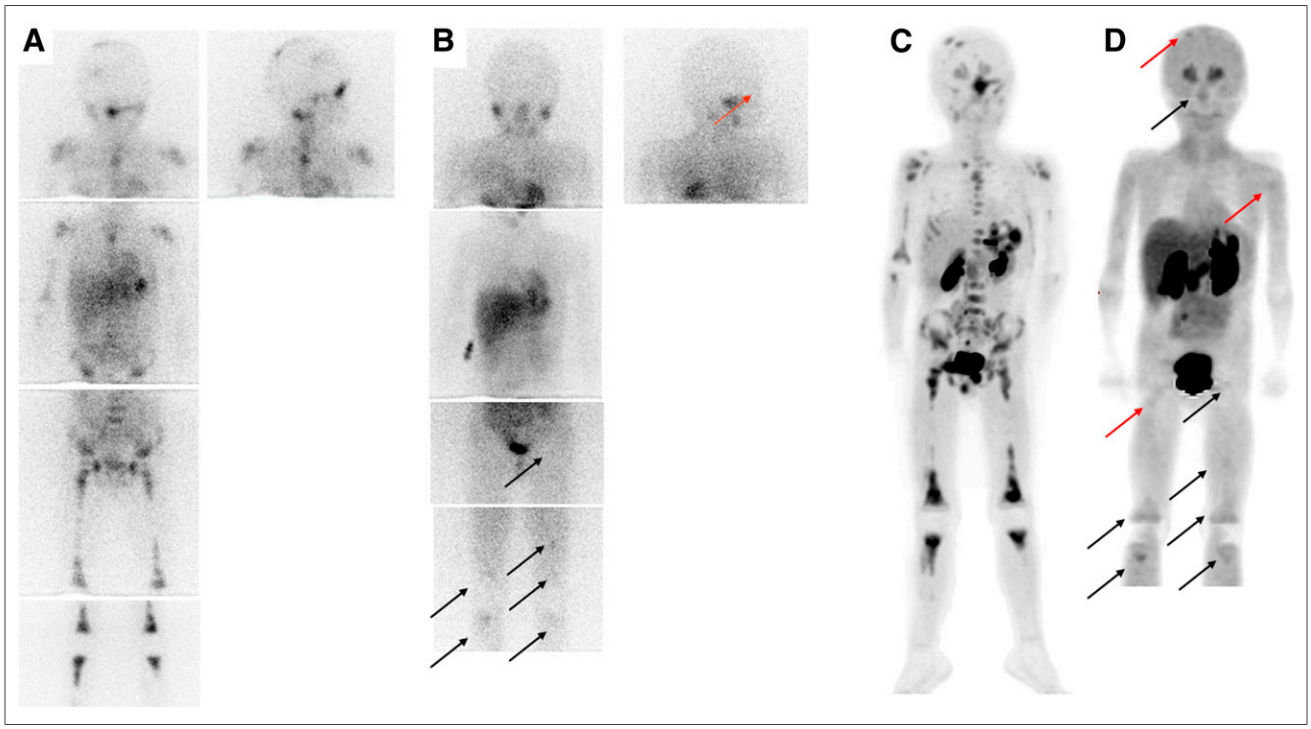

FIGURE 3. A 4-y-old child with stage 4 neuroblastoma (not MYCN-amplified) of abdominal primary. (A and C) At time of first staging, both ^{123}I-MIBG WBS (A) and ^{18}F-DOPA PET/CT with additional SPECT/CT (C) clearly showed primary tumor and diffuse bone or bone-marrow metastases. (B and D) After induction chemotherapy, both techniques identified some residual bone-marrow metastases (black arrows) but ^{18}F-DOPA PET/CT (maximum-intensity projection) revealed 3 small, persistent bone-marrow metastases (red arrows) not seen on ^{123}I-MIBG WBS.

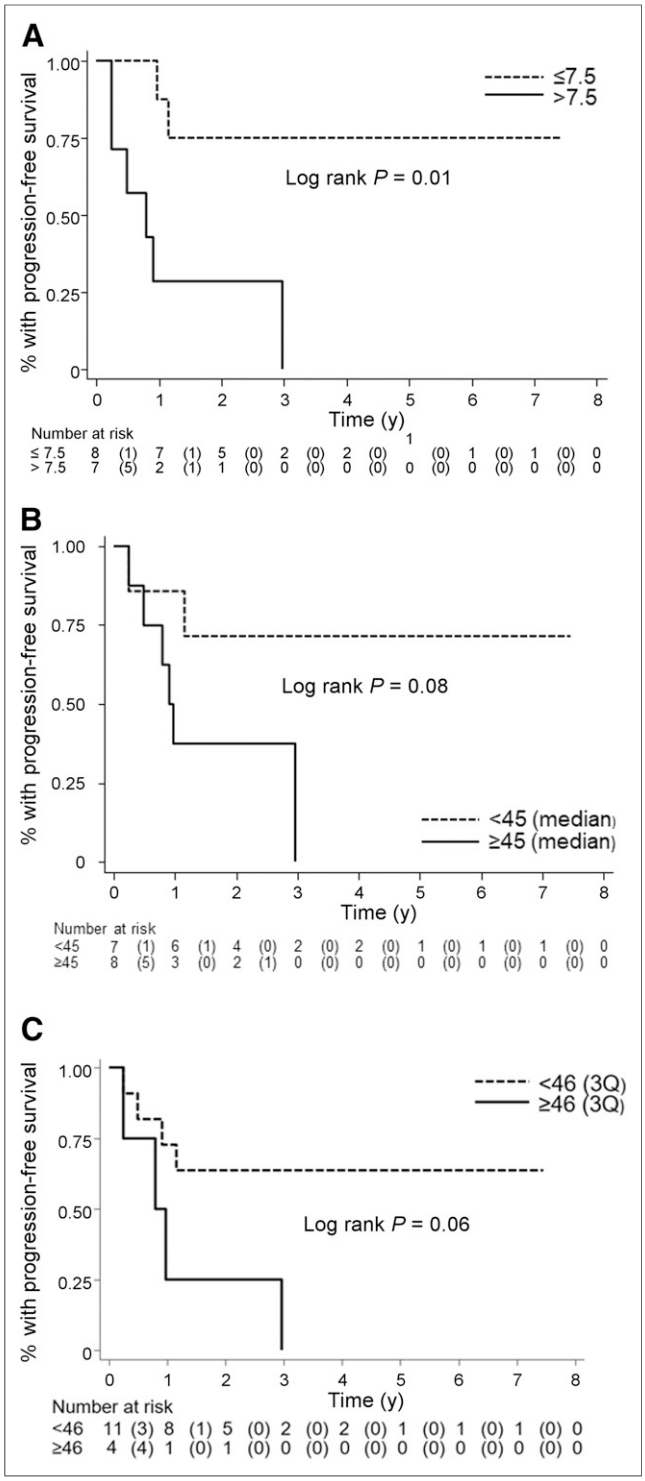

FIGURE 4. Kaplan–Meier PFS curves according to ^{18}F-DOPA WBMB ≤ 7.5 and > 7.5 after induction chemotherapy (A), ^{18}F-DOPA WBMB (median) ≤ 45 and > 45 before therapy (B), and ^{123}I-MIBG WBS score (third quartile) ≤ 46 and > 46 before therapy (C).

in the prognostic analysis. In this context, we did not find any associations between the different risk factors and OS. Indeed, we used PFS alone as a surrogate of prognosis.

In addition, a single stage 4 ^{123}I-MIBG–negative patient was included in the study. SPECT/CT images were coregistered and fused by means of appropriate software but were not acquired by means of a dedicated hybrid SPECT/CT system. This procedure is not optimal, as it does not provide the improved image quality yielded by CT attenuation correction. These issues may have caused the well-known diagnostic and prognostic power of the ^{123}I-MIBG scanning to be underestimated in this group of patients. In addition, the ^{18}F-DOPA WBMB score is characterized by high variability, as a result of the high intrinsic sensitivity of PET/CT procedures and the possibility of expressing the extent of soft-tissue metastases and uptake intensity; ^{18}F-DOPA WBMB therefore provides adequate information about patient risk, which may not be fully estimated by the ^{123}I-MIBG score.

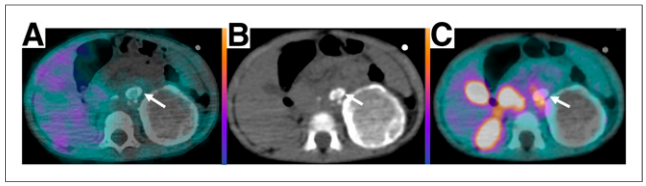

FIGURE 5. A 2-y-old child with stage III neuroblastoma (MYCN-amplified) of abdominal primary. Primary tumor was large and calcified at time of first staging, with major lymph node involvement. On axial images after induction chemotherapy (A–C; B is the CT component of SPECT/CT and PET/CT), large residual mass did not show any ^{123}I-MIBG or ^{18}F-DOPA uptake. However, some calcific lymph nodes negative on ^{123}I-MIBG SPECT/CT were still evident on ^{18}F-DOPA PET/CT (arrows). After induction chemotherapy, ^{123}I-MIBG WBS was <3 (i.e., 0) but WMBM was >7.5 (i.e., 16). By end of follow-up (19 mo), patient had died of disease progression.

However, to our knowledge, this is the first paper to prospectively analyze the diagnostic and prognostic role of ^{18}F-DOPA PET/CT in a well-selected population of children (median age, 28 mo) with high- and intermediate-risk neuroblastoma. Indeed, our preliminary data suggest that this tracer is more effective than ^{123}I-MIBG for the staging, treatment response evaluation, and prognostication of neuroblastoma patients.

In any case, to better evaluate the role of these 2 tracers in neuroblastoma, a direct comparison between ^{18}F-DOPA and ^{124}I-MIBG should be conducted. Such an analysis would eliminate any bias related to the different imaging procedures presented in this study.

Finally, although ^{123}I-MIBG scanning seems to be less sensitive than ^{18}F-DOPA PET/CT, the principal advantage of ^{123}I-MIBG remains its intrinsic theragnostic property. Although considering that the pathologic distribution of the tracers seems to be similar (*17,18,28*), there are not sufficient data to support the possibility of selecting patients for ^{123}I-MIBG therapy by using ^{18}F-DOPA PET/CT. From this point of view, ^{18}F-DOPA cannot replace ^{123}I-MIBG.

CONCLUSION

Our results confirmed good agreement between ^{18}F-DOPA PET/CT semiquantification and ^{123}I-MIBG scanning in neuroblastoma patients at the time of first staging, in that a positive correlation between the 2 techniques was observed. However, to stage neuroblastoma patients and, particularly, to evaluate disease persistence after induction chemotherapy, ^{18}F-DOPA PET/CT appears to be more sensitive than ^{123}I-MIBG WBS with additional SPECT/CT. In time-to-event analyses, ^{18}F-DOPA WBMB, evaluated after induction chemotherapy, remained the only risk factor independently and directly associated with disease progression. Further confirmation on a larger group of patient is required.

DISCLOSURE

No potential conflict of interest relevant to this article was reported.

KEY POINTS

QUESTION: Is ^{18}F DOPA PET/CT able to identify, after induction chemotherapy, neuroblastoma patients with persistence of disease at higher risk of disease progression?

PERTINENT FINDINGS: In a clinical study including 18 neuroblastoma patients at high and intermediate risk, ^{18}F-DOPA PET/CT was a reliable diagnostic tool for evaluating treatment response after induction chemotherapy and provided important information on the presence of disease persistence. Specifically, ^{18}F-DOPA PET/CT proved to be significantly more sensitive than ^{123}I-MIBG SPECT/CT in disclosing small and faint persistent bone and bone-marrow foci of pathologic uptake after chemotherapy.

IMPLICATIONS FOR PATIENT CARE: When compared with other prognostic factors and molecular imaging procedures, ^{18}F-DOPA PET/CT, performed after induction chemotherapy, was able to better identify patients at very high risk amenable to further effective treatments.

REFERENCES

1. London WB, Castleberry RP, Matthay KK, et al. Evidence for an age cutoff greater than 365 days for neuroblastoma risk group stratification in the Children's oncology group. *J Clin Oncol.* 2005;23:6459–6465.
2. Moroz V, Machin D, Faldum A, et al. Changes over three decades in outcome and the prognostic influence of age-at-diagnosis in young patients with neuroblastoma: a report from the international neuroblastoma risk group project. *Eur J Cancer.* 2011;47:561–571.
3. Seeger RC, Brodeur GM, Sather H, et al. Association of multiple copies of the N-myc oncogene with rapid progression of neuroblastomas. *N Engl J Med.* 1985;313:1111–1116.
4. Shimada H, Stram DO, Chatten J, et al. Identification of subsets of neuroblastomas by combined histopathologic and N-myc analysis. *J Natl Cancer Inst.* 1995;87:1470–1476.
5. Simon T, Hero B, Faldum A, et al. Long term outcome of high-risk neuroblastoma patients after immunotherapy with antibody ch14.18 or oral metronomic chemotherapy. *BMC Cancer.* 2011;11:21.
6. Valteau-Couanet D, Le Deley MC, Bergeron C, et al. Long-term results of the combination of the N7 induction chemotherapy and the busulfan-melphalan high dose chemotherapy. *Pediatr Blood Cancer.* 2014;61:977–981.
7. Matthay KK, Reynolds CP, Seeger RC, et al. Long-term results for children with high-risk neuroblastoma treated on a randomized trial of myeloablative therapy followed by 13-cis-retinoic acid: a children's oncology group study. *J Clin Oncol.* 2009;27:1007–1013.
8. Ladenstein R, Lambert B, Pötschger U, et al. Validation of the mIBG skeletal SIOPEN scoring method in two independent high-risk neuroblastoma populations: the SIOPEN/HR-NBL1 and COG-A3973 trials. *Eur J Nucl Med Mol Imaging.* 2018;45:292–305.
9. Lewington V, Lambert B, Poetschger U, et al. ^{123}I-mIBG scintigraphy in neuroblastoma: development of a SIOPEN semi-quantitative reporting, method by an international panel. *Eur J Nucl Med Mol Imaging.* 2017;44:234–241.
10. Bar-Sever Z, Biassoni L, Shulkin B, et al. Guidelines on nuclear medicine imaging in neuroblastoma. *Eur J Nucl Med Mol Imaging.* 2018;45:2009–2024.
11. Bonnin F, Lumbroso J, Tenenbaum F, Hartmann O, Parmentier C. Refining interpretation of MIBG scans in children. *J Nucl Med.* 1994;35:803–810.
12. Pfluger T, Piccardo A. Neuroblastoma: MIBG imaging and new tracers. *Semin Nucl Med.* 2017;47:143–157.
13. Piccardo A, Lopci E. Potential role of ^{18}F-DOPA PET in neuroblastoma. *Clin Transl Imaging.* 2016;4:79–86.
14. Kong G, Hofman MS, Murray WK, et al. Initial experience with gallium-68 DOTA-octreotate PET/CT and peptide receptor radionuclide therapy for pediatric patients with refractory metastatic neuroblastoma. *J Pediatr Hematol Oncol.* 2016;38:87–96.
15. Alexander N, Vali R, Ahmadzadehfar H, Shammas A, Baruchel S. Review: The role of radiolabeled DOTA-conjugated peptides for imaging and treatment of childhood neuroblastoma. *Curr Radiopharm.* 2018;11:14–21.
16. Cistaro A, Quartuccio N, Caobelli F, et al. ^{124}I-MIBG: a new promising positron-emitting radiopharmaceutical for the evaluation of neuroblastoma. *Nucl Med Rev Cent East Eur.* 2015;18:102–106.
17. Piccardo A, Lopci E, Conte M, et al. Comparison of ^{18}F-dopa PET/CT and ^{123}I-MIBG scintigraphy in stage 3 and 4 neuroblastoma: a pilot study. *Eur J Nucl Med Mol Imaging.* 2012;39:57–71.
18. Piccardo A, Puntoni M, Lopci E, et al. Prognostic value of ^{18}F-DOPA PET/CT at the time of recurrence in patients affected by neuroblastoma. *Eur J Nucl Med Mol Imaging.* 2014;41:1046–1056.
19. Lopci E, Piccardo A, Nanni C, et al. ^{18}F-DOPA PET/CT in neuroblastoma comparison of conventional imaging with CT/MR. *Clin Nucl Med.* 2012;37:e73–e78.
20. Lu MY, Liu YL, Chang HH, et al. National Taiwan University Neuroblastoma Study Group characterization of neuroblastic tumors using ^{18}F-FDOPA PET. *J Nucl Med.* 2013;54:42–49.
21. Lassmann M, Biassoni L, Monsieurs M, Franzius C, Jacobs F; EANM Dosimetry and Paediatrics Committees. The new EANM paediatric dosage card. *Eur J Nucl Med Mol Imaging.* 2007;34:796–798.
22. Matthay KK, Shulkin B, Ladenstein R, et al. Criteria for evaluation of disease extent by ^{123}I-metaiodobenzylguanidine scans in neuroblastoma: a report for the International Neuroblastoma Risk Group (INRG) Task Force. *Br J Cancer.* 2010;102:1319–1326.
23. Olivier P, Colarinha P, Fettich J, et al. Guidelines for radioiodinated MIBG scintigraphy in children. *Eur J Nucl Med Mol Imaging.* 2003;30:B45–B50.
24. Matthay KK, Edeline V, Lumbroso J, et al. Correlation of early metastatic response by^{123}I-metaiodobenzylguanidine scintigraphy with overall response and event-free survival in stage IV neuroblastoma. *J Clin Oncol.* 2003;21:2486–2491.
25. Fiebrich HB, Brouwers AH, Kerstens MN, et al. 6-[F-18]fluoro-L-dihydroxyphenylalanine positron emission tomography is superior to conventional imaging with ^{123}I-metaiodobenzylguanidine scintigraphy, computer tomography, and magnetic resonance imaging in localizing tumors causing catecholamine excess. *J Clin Endocrinol Metab.* 2009;94:3922–3930.
26. Berkowitz A, Basu S, Srinivas S, Sankaran S, Schuster S, Alavi A. Determination of whole-body metabolic burden as a quantitative measure of disease activity in lymphoma: a novel approach with fluorodeoxyglucose-PET. *Nucl Med Commun.* 2008;29:521–526.
27. Park JR, Bagatell R, Cohn SL, et al. Revisions to the International Neuroblastoma Response Criteria: a consensus statement from the National Cancer Institute clinical trials planning meeting. *J Clin Oncol.* 2017;35:2580–2587.
28. Piccardo A, Lopci E, Conte M, et al. Bone and lymph node metastases from neuroblastoma detected by ^{18}F-DOPA-PET/CT and confirmed by posttherapy ^{131}I-MIBG but negative on diagnostic ^{123}I-MIBG scan. *Clin Nucl Med.* 2014;39:e80–e83.